Available online at www.sciencedirect.com
SCIENCE DIRECT®
Journal of Solid State Chemistry 178 (2005) 270–278
JOURNAL OF SOLID STATE CHEMISTRY
www.elsevier.com/locate/jssc

# Crystal structure and thermal expansion of $PrGaO_3$ in the temperature range 12–1253 K

L. Vasylechko[a,*], Ye. Pivak[a], A. Senyshyn[a], D. Savytskii[a], M. Berkowski[b], H. Borrmann[c], M. Knapp[d], C. Paulmann[e]

[a]*Institute of Telecommunications, Radioelectronics and Electronics Technique,"Lviv Polytechnic" National University, 12 Bandera St., UA-79013 Lviv, Ukraine*
[b]*Institute of Physics Polish Academy of Sciences, Al. Lotników 32/46, 02-668 Warsaw, Poland*
[c]*Max-Planck-Institut für Chemische Physik fester Stoffe, Nöthnitzer Strasse 40, D-01187 Dresden, Germany*
[d]*Institute for Materials Science, Darmstadt University of Technology, Petersenstrasse 23, D-64287 Darmstadt, Germany*
[e]*Mineralogisch-Petrographisches Institut, Universität Hamburg, Grindelallee 48, D-20146 Hamburg, Germany*

Received 20 August 2004; received in revised form 29 September 2004; accepted 4 October 2004

**Abstract**

Crystal structure and thermal expansion of $PrGaO_3$ single crystal, obtained by the Czochralsky method, have been investigated by means of single crystal and high-resolution powder diffraction techniques applying synchrotron radiation in a wide temperature range 12–1253 K. It was shown that $PrGaO_3$ adopts an orthorhombically distorted variant of perovskite structure ($GdFeO_3$ type of structure, space group *Pbnm*, $Z = 4$) throughout the entire temperature range. Temperature dependence of lattice parameters and respective unit cell volume display anisotropic and nonlinear behavior. Lattice contraction in [010]- and [100]-directions is observed in temperature ranges 12–180 and 12–50 K, respectively. In total $PrGaO_3$ exhibits a negative thermal expansion of the volume between 12 and 50 K. A linear increase of the average bond lengths $(PrO)_8$, $(PrO)_9$, $(PrO)_{12}$, $(GaO)_6$, as well as the average $(OO)_8$ distances was observed. However, with the average $(PrPr)_6$, $(PrGa)_8$ and $(GaGa)_6$ cation–cation distances a change of slope occurs at 200–300 K. Over all, with rising temperature a decrease of the deformation is observed for the perovskite type structure. A phase transition from orthorhombic to rhombohedral structure of $PrGaO_3$ around 1855 K is predicted from extrapolation of both the temperature dependencies of the $(PrPr)_6/(GaGa)_6$ distance ratio and of the experimental temperatures of the $R\bar{3}c$–*Pbnm* phase transition for $LaGaO_3$, $CeGaO_3$ and $La_{1-x}RE_xGaO_3$ (*RE*—rare earth) perovskites.


*Keywords:* $PrGaO_3$; Single crystal; Perovskite; Crystal structure; Negative thermal expansion; Phase transition; Synchrotron radiation

## 1. Introduction

Rare-earth gallates, due to their particular properties, have found wide application in different areas of science and engineering. In particular, $NdGaO_3$, $LaGaO_3$, $PrGaO_3$ as well as respective solid solutions are used as substrate materials for epitaxial growth of high-temperature superconductors (HTSC), collosal magnetoresistive films and for GaN film deposition [1–6]. A small lattice mismatch, similar coefficients of thermal expansion, high thermal and chemical stability, and in particular only small misfits at epitaxial growth temperatures are all-important features in growing layers of HTSC materials. Recently, it was reported [7–10], that lanthanum, neodymium and praseodymium gallates, doped with strontium and magnesium show high oxygen ion conductivity at temperatures of about 870–1070 K, and are considered as prospective solid electrolytes for the application in solid oxide fuel cells (SOFCs).

At ambient temperatures $PrGaO_3$ adopts an orthorhombically distorted $GdFeO_3$-type structure (space

*Corresponding author. Fax: +38 322 742164.
*E-mail address:* crystal-lov@polynet.lviv.ua (L. Vasylechko).

0022-4596/$ - see front matter © 2004 Elsevier Inc. All rights reserved.
doi:10.1016/j.jssc.2004.10.005

group *Pbnm*). This structure remains unchanged down to 12 K [11,12]. High temperature structural investigations of $PrGaO_3$ have so far been limited to measurements of lattice parameters at certain temperatures within the temperature range 300–1270 K [2,3,13,14]. To our knowledge, there are no data on structural refinement of $PrGaO_3$ at elevated temperatures in the literature. The data on possible phase transformations in $PrGaO_3$ are contradictory. A second-order transition was observed by DTA and DSC methods at 1090 K, although this transformation could not be correlated with a structural change [14]. Based on X-ray diffraction experiments and thermal analyses Sasaura et al. [15] suggested the existence of a phase transition, presumably orthorhombic–rhombohedral, above 1670 K. Finally, differential thermal analyses performed by Miyazawa et al. [3], did not confirm the existence of a second-order phase transition in $PrGaO_3$ around 1090 K, as reported in Ref. [14], but presented a first-order-like transition at ~1850 K, very close to the melting temperature.

The present paper is devoted to detailed structure investigation of $PrGaO_3$ performed in situ in a wide temperature range between 12 and 1253 K by means of single-crystal and high-resolution powder diffraction (HRPD) techniques applying conventional X-ray and synchrotron radiation. This work is a continuation in our systematic studies of the structures and phase transitions in $REGaO_3$ perovskites (*RE*—rare earths). Some preliminary results on the room-temperature structure of $PrGaO_3$ and low-temperature behavior of the lattice parameters in the temperature range of 12–300 K have been published already in our communications [16–19]. This work supplements the previously published data with the results of the in situ high-temperature investigation of the $PrGaO_3$ structure. The crystallographic analysis of all structural parameters is made in a wide temperature range investigated.

## 2. Experimental

A single crystal of $PrGaO_3$ was grown by the Czochralsky method. Details of the growth procedure have already been described [20]. X-ray phase analysis of the powdered sample of $PrGaO_3$ sample ensured a perovskite-type structure of $PrGaO_3$; reflections of other phases were not revealed. Crystal structure and thermal expansion of the crystal have been investigated by means of single crystal and HRPD techniques using synchrotron radiation in a wide temperature range of 12–1253 K. For the structure determination, a twin-free single domain plate-like shaped crystal was selected from a single crystal boule after careful examination.

X-ray synchrotron diffraction data were collected at beamline F1 (HASYLAB/DESY) with a wavelength of 0.565 Å and a sample–detector distance of 30.0 mm using a Smart 1 K CCD system and an Oxford Cryostream cooling device. The data collection was performed with Omega-scans ($\Delta\omega = 0.1^\circ$, $t = 2-10$ s) at 8 different $\varphi$-settings giving a data set of 6303 reflections with a calculated min/mean/max redundancy of 14.625/9/28 and 100% coverage (*mmm* symmetry) up to a resolution of 0.495 Å. The typical FWHM of the reflections was 0.05°. The lattice parameters were calculated using the orientation matrices incorporating correction factors (diffractometer zeros, CCD camera miss setting, etc.). The integration was performed with SAINT using an integration box size of $xy/z = 2.0^\circ/0.12^\circ$. A correction for systematic errors, absorption and scaling was done using SADABS by fitting spherical harmonic functions following the method of Blessing [21]. The structure determination and refinement was carried out using the program package WinCSD [22].

The low temperature behavior of the $PrGaO_3$ structure in the temperature range 12–300 K has been studied by means of powder diffraction technique using a laboratory X-ray source as well as synchrotron radiation. In both cases a He closed-cycle cryostat was used. X-ray powder diffraction patterns were collected by using a Guinier transmission camera (HUBER image plate, Cu$K\alpha_1$ radiation) in $2\theta$ range 4–100°. Two sets of data were collected with a temperature step of 10/20 K during cooling and heating. HRPD experiments using synchrotron radiation have been performed at the powder diffractometer at beamline B2 (HASYLAB, DESY). For beam conditioning a cylindrically curved X-ray mirror, a Ge(111) double-crystal monochromator and a Ge(111) crystal analyser in front of a NaI scintillation counter were inserted. The wavelength was calibrated using the positions of five silicon reflections (NIST640b). Full diffraction patterns were collected at 12 K ($2\theta$ range 14–77°, $\Delta 2\theta = 0.006^\circ$, $\lambda = 1.11972$ Å) and 95 K ($2\theta$ range 16.5°–69°, $\Delta 2\theta = 0.004^\circ$, $\lambda = 1.13973$ Å). In order to obtain the thermal behavior of the lattice parameters, the measurements of the thermal evolution of 14 characteristic reflections were carried out in the temperature range 12–300 K. To obtain precise reflection positions, the intensities and FWHM values of every peak, the experimental profiles were fitted using the profile decomposition program PROFAN [22]. Lattice parameters were refined by least-squares method taking into account the refinement of the "zero shift" values.

High temperature (HT) structure investigations in the temperature range 300–1250 K were performed applying high-resolution powder diffraction technique and synchrotron radiation by using a newly developed on-site readable image plate detector (*OBI*) [23]. A 0.3 mm quartz capillary was filled with powdered $PrGaO_3$ specimen and mounted inside a STOE furnace in Debye–Scherrer geometry, equipped with a

EUROTHERM temperature controller and a capillary spinner. Full patterns were collected over a $2\theta$ range of 7.48° to 85° with a step size 0.004° at RT, 373, 473, 573, 673, 773, 873, 973, 1073, 1173, 1223, 1243 and 1253 K. The wavelength was selected close to Mo$K\alpha_1$ and was determined to be 0.70879(5) Å based on 6 reflections of Si standard NIST640b.

Full profile Rietveld method was used for the refinement of the lattice parameters, positional and displacement parameters of atoms. The data evaluation was performed by using the WinCSD program package [22].

## 3. Results and discussion

### 3.1. Crystal structure

Analysis of reflection conditions in the single crystal experimental data set, collected at RT, revealed two possible space groups: *Pbnm* and $Pbn2_1$. Full-matrix least-squares refinement of the structure with anisotropic approximation of displacement parameters for all atoms, performed in space group *Pbnm* by using 788 averaged reflections with $F > 4\sigma(F)$, resulted in reability factors of $R_F = 0.027$ and $R_W = 0.026$. Refinement in space group $Pbn2_1$ did not lead to improvement of the residuals: $R_F = 0.029$, $R_W = 0.029$ for 1093 reflections. Besides, physically meaningless values of anisotropic displacement parameters for oxygen atoms were obtained in this structural model. Therefore, the centrosymmetric space group *Pbnm* was chosen for the final description of the $PrGaO_3$ structure. Final results of the structure refinement of $PrGaO_3$ are summarized in Table 1, corresponding interatomic distances and angles in Table 2. Projection of the $PrGaO_3$ structure at RT into the *ab*-plane is shown in Fig. 1.

The Ga atoms in the $PrGaO_3$ structure are located in the centers of almost regular corner-shared $GaO_6$ octahedra which form a 3-D network. Deformed cubo-octahedral holes of this grid of octahedra are occupied by praseodymium atoms, which are surrounded by eight oxygen atoms at distances 2.37–2.73 Å and four additional O-atoms at 3.06–3.28 Å.

The study of the $PrGaO_3$ structure by using HRPD technique and synchrotron radiation in the temperature range of 12–1253 K confirmed that $PrGaO_3$ structure remains orthorhombic in the whole temperature range investigated. As examples, the graphical results of the Rietveld refinement of the $PrGaO_3$ structure at 12 and 1253 K are presented in Fig. 2.

### 3.2. Thermal expansion

Analysis of the thermal behavior of the lattice parameters, obtained from powder data collected with a laboratory X-ray source, revealed a strong anisotropy in the thermal expansion in different directions. A negative thermal expansion in *b*-direction was observed in the temperature range 12–180 K. To study this anomaly in more detail, HRPD technique and synchrotron radiation were applied. Extremely high beam collimation (typical FWHM values are 0.01–0.02°) and good signal-to-noise ratio allowed us to observe the line splitting, which could not be observed in conventional X-ray patterns (Fig. 3). Analysis of the character of the splitting and absence of superstructure reflections in the pattern collected at 12 K indicate that there are no structural changes in this temperature range. Fig. 4 shows the temperature dependencies of the cell parameters and relative lattice expansion in the temperature range 12–1253 K. There is an anomaly in the thermal expansion at low temperatures. Negative expansion in [010] and [100] directions is observed in the temperature ranges 12–180 and 12–50 K, respectively. As a result, in the temperature range 12–50 K a decrease of the cell volume occurs with rising temperature. Observed

Table 1
Structural parameters of $PrGaO_3$ at ambient temperature (space group *Pbnm*, $Z = 4$, $a = 5.4557(1)$ Å, $b = 5.4901(1)$ Å, $c = 7.7275(2)$ Å)

| Atom, sites | $x$ | $y$ | $z$ | $B_{iso/eq}$[a] (Å$^2$) | | |
|---|---|---|---|---|---|---|
| Pr, 4*c* | −0.00742(2) | 0.03522(3) | $\frac{1}{4}$ | 0.417(8) | | |
| Ga, 4*b* | $\frac{1}{2}$ | 0 | 0 | 0.30(2) | | |
| O1, 4*c* | 0.0758(4) | 0.4848(4) | $\frac{1}{4}$ | 0.48(3) | | |
| O2, 8*d* | −0.2868(2) | 0.2871(2) | 0.0404(2) | 0.41(2) | | |
| | Anisotropic displacement parameters of atoms | | | | | |
| | $B_{11}$ | $B_{22}$ | $B_{33}$ | $B_{12}$ | $B_{13}$ | $B_{23}$ |
| Pr, 4*c* | 0.37(1) | 0.59(2) | 0.30(1) | −0.055(2) | 0 | 0 |
| Ga, 4*b* | 0.24(3) | 0.45(2) | 0.22(3) | 0.01(1) | −0.02(1) | −0.06(3) |
| O1, 4*c* | 0.47(6) | 0.81(5) | 0.14(3) | 0.01(4) | 0 | 0 |
| O2, 8*d* | 0.40(3) | 0.42(3) | 0.42(3) | −0.15(3) | 0.06(2) | −0.04(3) |

[a] $B_{iso/eq} = 1/3[B_{11}(a^*)^2a^2 + \cdots + 2B_{23}b^*c^*bc\cos a]$; $T = \exp[-1/4(B_{11}(a^*)^2h^2 + \cdots + 2B_{23}b^*c^*kl)]$.

Table 2
Selected interatomic distances and angles in $PrGaO_3$ at room temperature

| Atoms | Distances (Å) | Atoms | Distances (Å) | Atoms | Angles (deg) |
|---|---|---|---|---|---|
| Pr–1O1 | 2.371(2) | Ga–2O2 | 1.978(1) | *b*O2–Ga–*b*O1 | 89.24(6) |
| Pr–2O2 | 2.396(1) | Ga–2O1 | 1.9774(5) | *b*O2–Ga–*a*O2 | 91.11(5) |
| Pr–1O1 | 2.509(2) | Ga–2O2 | 1.984(1) | *b*O2–Ga–*b*O2 | 88.89(5) |
| Pr–2O2 | 2.619(1) | | | *a*O1–Ga–*b*O1 | 180.00(7) |
| Pr–2O2 | 2.727(1) | Ga–2Ga | 3.8637(2) | *a*O1–Ga–*a*O2 | 90.10(6) |
| Pr–1O1 | 3.056(2) | Ga–4Ga | 3.8699(1) | *a*O1–Ga–*b*O2 | 89.90(6) |
| Pr–1O1 | 3.113(2) | | | *b*O1–Ga–*a*O2 | 89.90(6) |
| Pr–2O2 | 3.277(1) | O1–2O2 | 2.777(2) | *b*O1–Ga–*b*O2 | 90.10(6) |
| | | O1–2O2 | 2.797(2) | *a*O2–Ga–*b*O2 | 180.00(5) |
| Pr–2Pr | 3.8134(2) | O1–2O2 | 2.805(2) | | |
| Pr–2Pr | 3.8839(2) | O1–2O2 | 2.816(2) | Ga–O1–Ga | 155.37(9) |
| Pr–2Pr | 3.9274(2) | | | Ga–O2–Ga | 155.33(7) |
| | | O2–2O2 | 2.774(2) | | |
| Pr–2Ga | 3.2008(2) | O2–2O2 | 2.828(2) | | |
| Pr–2Ga | 3.3154(2) | | | | |
| Pr–2Ga | 3.3813(2) | | | | |
| Pr–2Ga | 3.5168(2) | | | | |

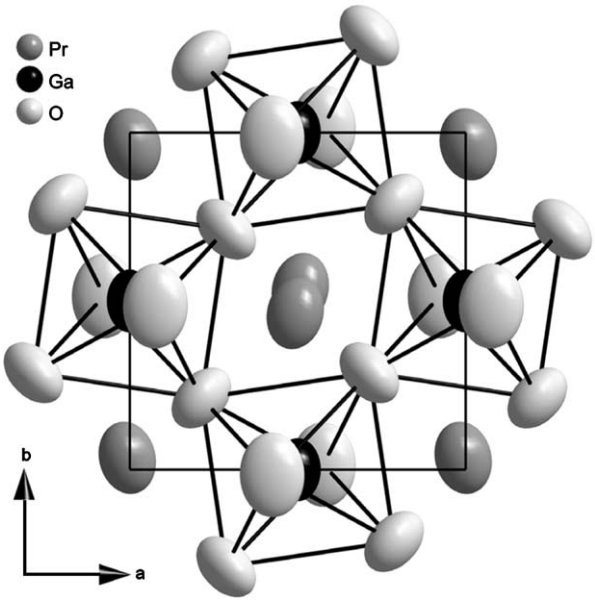


Fig. 1. The projection of the $PrGaO_3$ structure at ambient temperature onto the *ab*-plane. Displacement ellipsoids of the atoms with a probability factor of 60% are shown.

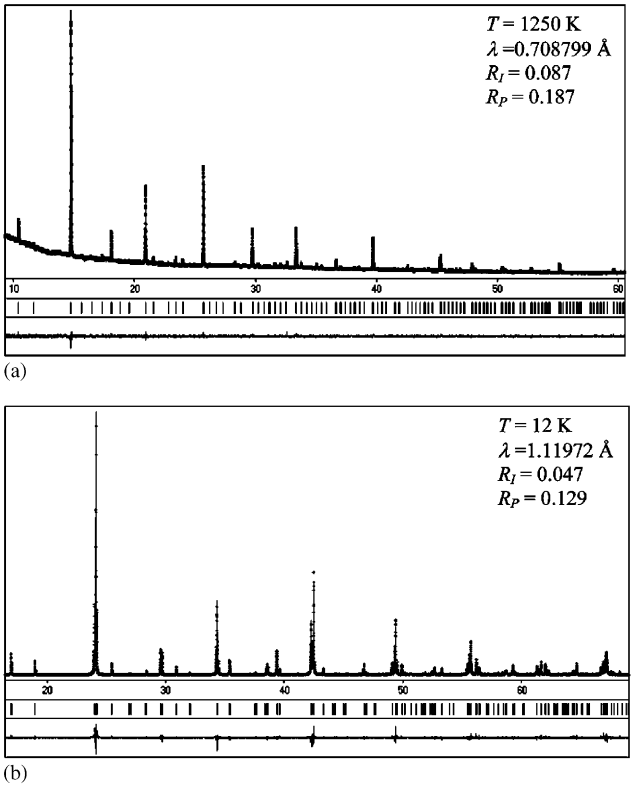


Fig. 2. Synchrotron powder diffraction patterns of $PrGaO_3$ at 1250 K ($\lambda = 0.708799$ Å, image plate *OBI* detector) and 12 K ($\lambda = 1.11972$ Å, scintillation NaI-detector) refined in space group *Pbnm*. Experimental and calculated patterns, difference profiles and positions of the diffraction maxima are given.

anomalies in the low temperature (LT) expansion can be attributed to an interaction between the phonon vibrations and electronic excitation of $Pr^{3+}$ ions [19].

The cell parameters increase nonlinearly and anisotropically with temperature. Maximal and practically equal relative expansion is observed in *a*- and *c*-directions, whereas relative expansion along *b*-axis is roughly 2 times lower (Fig. 4). Due to anisotropy of thermal expansion, the values of pseudocubic perovskite-like parameters, defined as $a_{pc} = \sqrt{(a_0^2 + b_0^2)}/2$ and $c_{pc} = c_0/2$, become equal near 894 K, whereas the shear angle $\gamma_{pc} = 2^{*}\text{arctg}(b_0/a_0)$ is equal to 89.81° at this

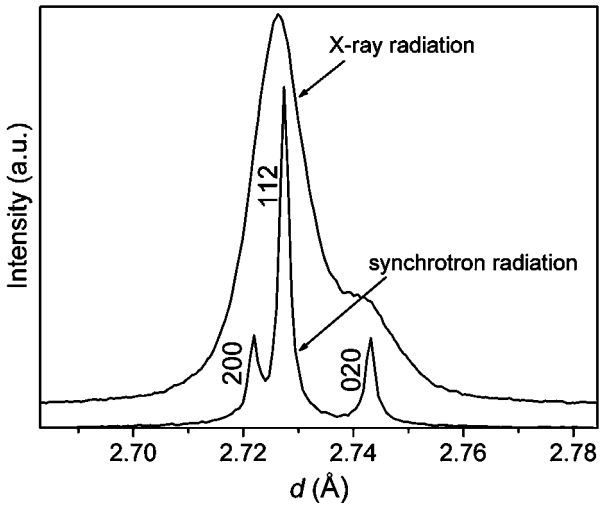


Fig. 3. Examples of the observed diffraction profiles of (200)+(112)+(020) triplet for $PrGaO_3$, measured at 12 K by using parallel beam geometry with analyser crystal and synchrotron radiation, compared with those obtained by using laboratory X-ray source (HUBER G670 Guinier camera, image plate, Cu$K\alpha_1$—radiation).

temperature. From the extrapolation of the lattice parameters it could be predicted that $a_0$ and $b_0$ lattice parameters become equal near 1523 K and the shear angle $\gamma_{pc}$ approaches ninety degrees. However, the $PrGaO_3$ lattice only becomes metrically tetragonal at this temperature. It is evident, that at the temperatures higher than 1523 K different cell parameter ratio, namely $a_0 > b_0$, is typical for $PrGaO_3$ structure. A similar cell parameter ratio ($a_0 > b_0$) is observed in related $LaGaO_3$ and $CeGaO_3$ structures below the $Pbnm-R\bar{3}c$ phase transitions, which occur at temperatures of 425 K [11,24] and 1250 K [25], respectively. Moreover, the analysis of the literature data shows that the majority of other $GdFeO_3$-type compounds with $a_0 > b_0$ parameter ratio ($SmAlO_3$ [26], $LaCrO_3$ [27], $PrNiO_3$ and $NdNiO_3$ [28]) undergo the phase transition from orthorhombic to rhombohedral structures at elevated temperatures. Evidently, if the $a_0 > b_0$ parameter ratio occurs in the perovskites with $GdFeO_3$ type of structure, it may serve as indication of the forthcoming phase transition from orthorhombic to rhombohedral structure. As shown below, such a phase transition in $PrGaO_3$ could be predicted near 1855 K.

An increase in temperature leads to a systematic increase of the eight shortest Pr–O distances, whereas a decrease of the four more remote Pr–O distances is observed (Fig. 5). From the distribution of Pr–O interatomic distances and their temperature behavior (Table 2, Fig. 5) it is evident, that a coordination number (CN) of 8 should be chosen for the Pr atoms in the temperature range 12–1000 K, whereas for the temperatures higher than 1000 K a CN of 10 looks more preferable.

The temperature dependency of the averaged interatomic distances in the $PrGaO_3$ structure are presented in Fig. 6. A linear increase of the average bond lengths $(PrO)_8$, $(PrO)_9$, $(PrO)_{10}$, $(PrO)_{12}$ and $(GaO)_6$, as well as of the $(OO)_8$ average distances is observed with increasing temperature. For the temperature dependencies of the average cation–cation distances a change of slope occurs at 200–300 K.

Increase in temperature leads to a decrease of the perovskite structure deformation for $PrGaO_3$, which is demonstrated by an increase of the *observed tolerance factors,* $t_{obs}$ (Fig. 7). The latter criterion was introduced by Sasaki et al. [29] for a description of structure deformation, arising from the tilts and/or distortions of polyhedra in perovskite-type structures. It is defined as follows: $t_{obs} = (AO)_{12}/\sqrt{2}(BO)_6$, where $(AO)_{12}$ and $(BO)_6$ are the average interatomic distances with a coordination of twelve and six for *A*- and *B*-sites, respectively. Temperature dependency of the values of $t_{obs}$, calculated for all reasonable CN of $Pr^{3+}$ ions, are shown in Fig. 7.

Analysis of the so-called *bond-length distortion* ($\Delta$) calculated according to Ref. [29] for the corresponding $PrO_8$–$PrO_{12}$ polyhedra also confirms the tendency for a decrease of the structure deformation and show that CNs of 8–10 are preferable for Pr atoms in the $PrGaO_3$ structure (Fig. 8). The $PrO_{12}$ cubooctahedron is much more distorted in comparison with $PrO_8$, $PrO_9$ and $PrO_{10}$ polyhedra.

Values of octahedra tilt angles, obtained from the experimental values of the Ga–O1–Ga and Ga–O2–Ga angles, have a tendency to decrease with rising temperature, indicating a decreasing distortion of the perovskite structure with temperature.

The ratio of the cation–cation distances could also serve for the characterization of the degree of deformation in the $ABO_3$ perovskite structures [30]. For the ideal cubic perovskite structure, as well as for the rhombohedral $R\bar{3}c$ structure, all individual *A*–*A* and *B*–*B* distances are the same and the ratio of the average $(AA)_6/(BB)_6$ interatomic distances should be equal to 1. Temperature dependency of the $(PrPr)_6/(GaGa)_6$ average distance ratio (Fig. 9) indicates the decrease of the orthorhombic deformation of the $PrGaO_3$ structure with temperature. From extrapolation of the temperature dependency of the $(PrPr)_6/(GaGa)_6$ distance ratio the transition from orthorhombic to rhombohedral structure could be predicted at a temperature of 1856 K. This value agrees very well with the temperature of the phase transformation in $PrGaO_3$ detected by DTA method [2]. Fig. 10 summarizes the transition temperatures reported already for the $LaGaO_3$, $CeGaO_3$, $La_{1-x}Nd_xGaO_3$, $La_{1-x}Pr_xGaO_3$, $La_{1-x}Sm_xGaO_3$, and $La_{1-x}Gd_xGaO_3$ perovskites [20,25,31–34], as well as for the newly investigated $La_{1-x}RE_xGaO_3$ ($RE$=Ce, Ho, Er, Y) systems. Shannon's ionic radii for the ninefold

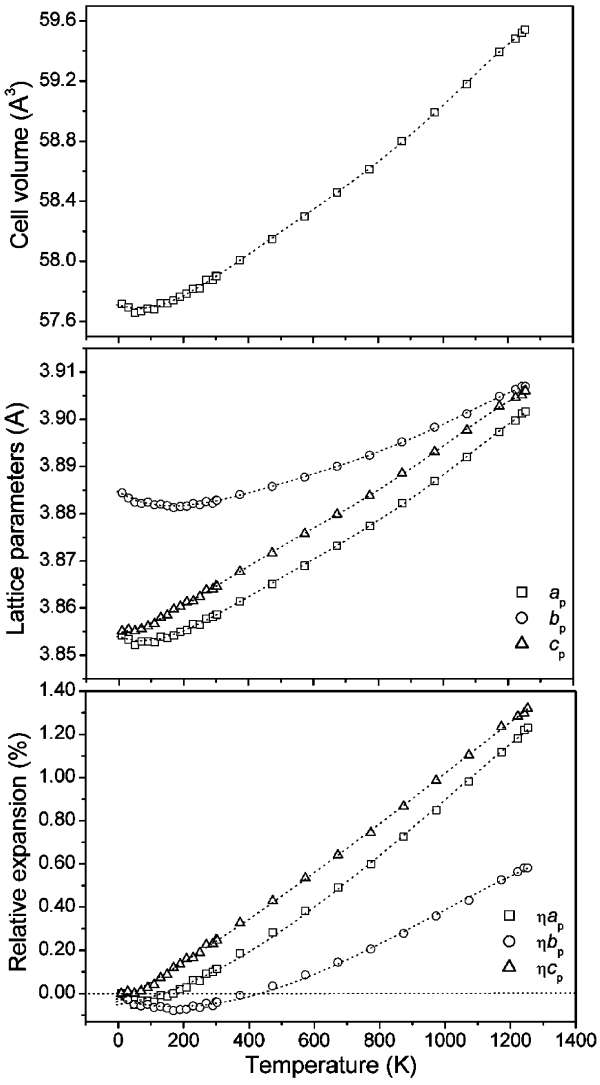


Fig. 4. Temperature dependencies of the lattice parameters and relative lattice expansion in $PrGaO_3$ structure. Lattice parameters of the orthorhombic phase are normalized to perovskite-like cell parameters as follows: $a_p = a_0/\sqrt{2}$, $b_p = b_0/\sqrt{2}$, $c_p = c_0/2$, $V_p = V_0/4$. Perovskite-like cell parameters change with temperature as follows:

$a_p = 3.8539 - 2.61 \times 10^{-5}T + 2.275 \times 10^{-7}T^2 - 3.748 \times 10^{-10}T^3 + 2.904 \times 10^{-13}T^4 - 8.27 \times 10^{-17}T^5$,
$b_p = 3.8845 - 4.09 \times 10^{-5}T + 1.821 \times 10^{-7}T^2 - 2.736 \times 10^{-10}T^3 + 2.045 \times 10^{-13}T^4 - 5.76 \times 10^{-17}T^5$,
$c_p = 3.8547 + 1.08 \times 10^{-5}T + 1.358 \times 10^{-7}T^2 - 2.655 \times 10^{-10}T^3 + 2.295 \times 10^{-13}T^4 - 7.09 \times 10^{-17}T^5$,
$V_p = 57.704 - 8.383 \times 10^{-4}T + 8.152 \times 10^{-6}T^2 - 1.365 \times 10^{-8}T^3 + 1.083 \times 10^{-11}T^4 - 3.161 \times 10^{-15}T^5$.
Relative thermal expansion is defined as follows:
$\eta a_p = ((a_p(T) - a_p(T_0))/a_p(T_0)) \times 100\%$,
$\eta b_p = ((b_p(T) - b_p(T_0))/b_p(T_0)) \times 100\%$,
$\eta c_p = ((c_p(T) - c_p(T_0))/c_p(T_0)) \times 100\%$.

coordinated $RE^{3+}$ cations were used [35]. From the linear extrapolation of the experimental data for $La_{1-x}RE_xGaO_3$ perovskites, the estimated temperature of the phase transition in $PrGaO_3$ is $T_c = 1855\,K$.

The temperature evolution of the isotropic atomic displacement parameters $U$ (*adps*) of the Pr-, Ga- and O-atoms, evaluated by the Rietveld method, is presented in Fig. 11. An overall mode of refinement of the *adp* values was applied for the two different oxygen sites. The slopes $dU/dT$ and the values of the *adps* in $PrGaO_3$ structure as derived from the synchrotron and X-ray diffraction data are in good agreement with the empirical sequence $U(O) > U(A) > U(B)$. This relation was obtained in [36] from the survey of more than 40 entries in the Inorganic Crystal Structure Database for $A^{III}B^{III}O_3$ type perovskites refined from neutron diffraction data.

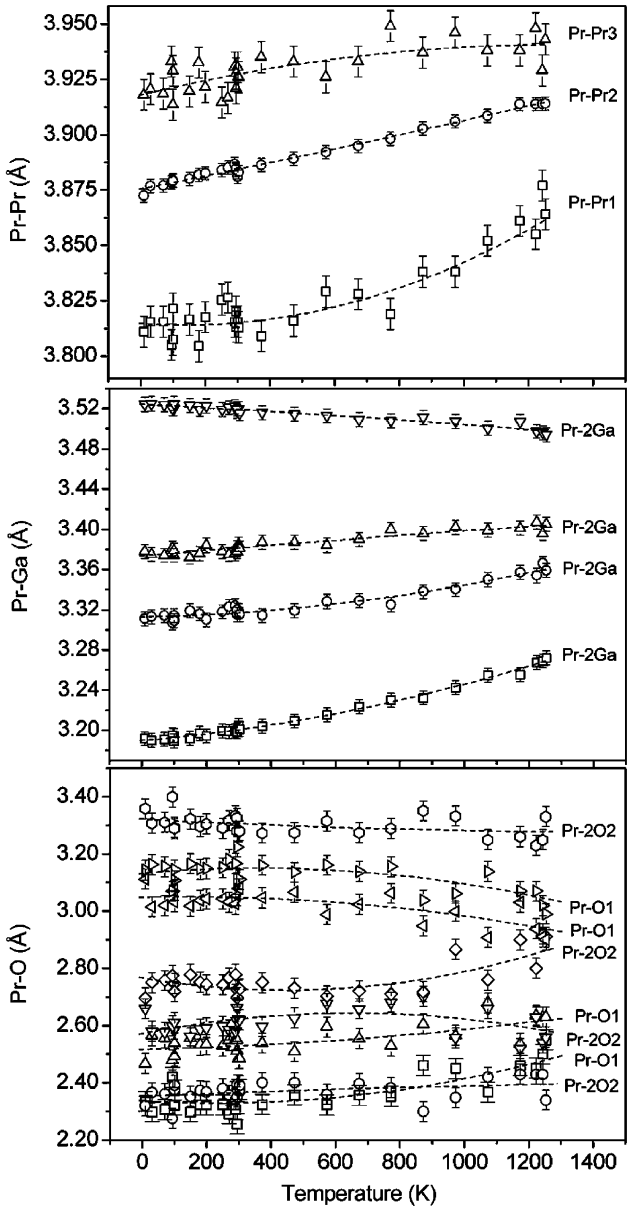


Fig. 5. Temperature dependencies of some interatomic distances in the $PrGaO_3$ structure. Experimental data points were fitted by second-order polynomials.

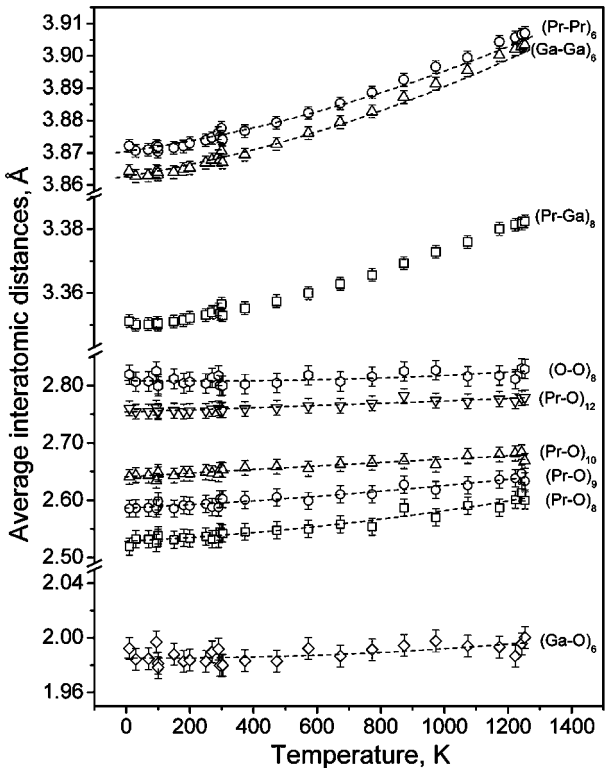


Fig. 6. Temperature dependency of the averaged interatomic distances in the $PrGaO_3$ structure. Data points were fitted by second-order polynomials.

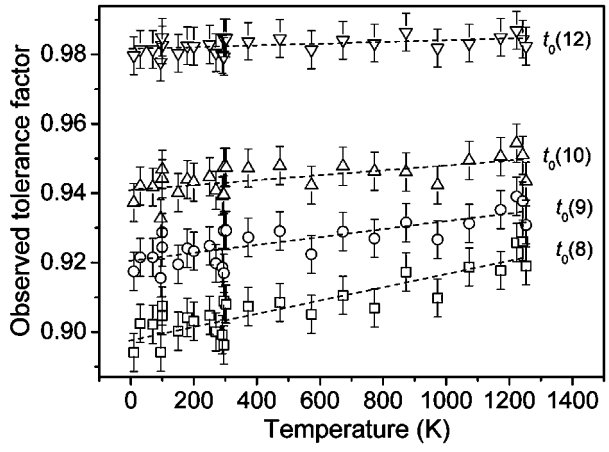


Fig. 7. Temperature dependency of the observed tolerance factor in $PrGaO_3$ structure, calculated for four reasonable coordination numbers of Pr atoms.

## 4. Conclusion

In the temperature range 12–1253 K praseodymium gallate $PrGaO_3$ exhibits an orthorhombically distorted $GdFeO_3$ type structure (space group *Pbnm*, $Z = 4$). Lattice parameters and cell volume display anisotropic nonlinear thermal behavior. Lattice contraction in [010]- and [100]-directions in the temperature ranges 12–180 and 12–50 K, respectively, leads to negative thermal volume expansion in the temperature range 12–50 K. $(PrO)_8$, $(PrO)_9$, $(PrO)_{12}$, $(GaO)_6$, and $(OO)_8$ average bond lengths increase linearly with temperature, whereas for the temperature dependency of the $(PrPr)_6$, $(PrGa)_8$ and $(GaGa)_6$ average distances a change of slope at 200–300 K occurs. With rising temperature, a decrease of the perovskite structure deformation is

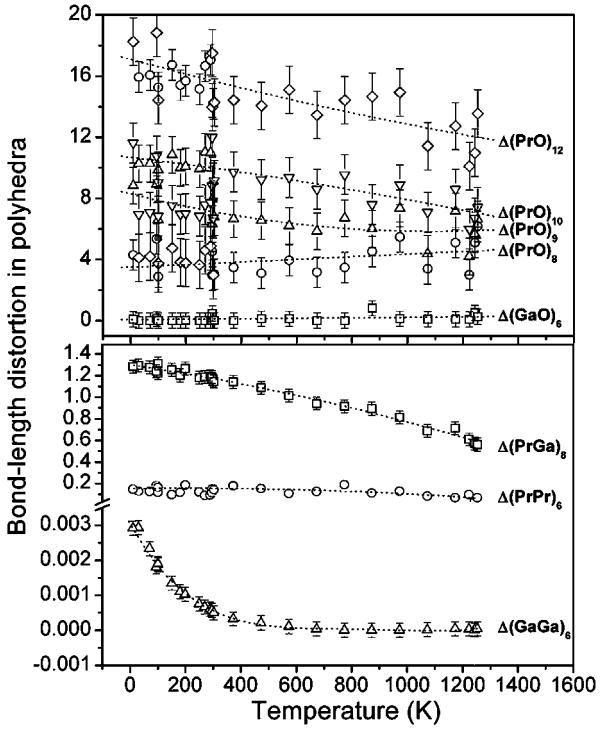


Fig. 8. Bond-length distortion of the polyhedra $\Delta$ in $PrGaO_3$ structure versus temperature. $\Delta = (1/n)\sum\{(r_i - \bar{r})/\bar{r}\}^2 \times 10^3$, where $r_i$ and $\bar{r}$—are the individual and average values of the interatomic distances in the polyhedra with coordination number $n$ [29].

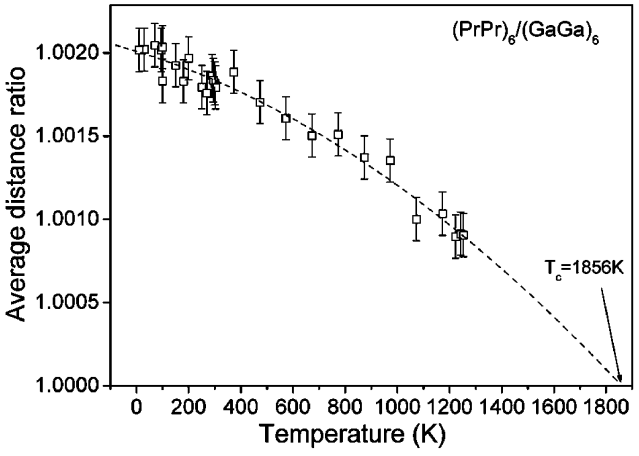


Fig. 9. Evaluation of $T_c$ of the orthorhombic-to-rhombohedral phase transition in $PrGaO_3$ from the temperature dependency of the average distance ratio $(PrPr)_6/(GaGa)_6$. Experimental data points were fitted by a second-order polynomial.

observed, which leads to a predicted *Pbnm–R*$\bar{3}$*c* phase transformation at 1856 K.

## Acknowledgments

The work was supported in part by WTZ (UKR-01/12), Ukrainian Ministry of Education and Sciences (Projects "Cation" and 85-2003), Polish Committee for Scientific Research (Grant No. 7 T08A 00520) and ICDD Grant-in-aid program. L.V. acknowledges the Max Planck Society for a research fellowship.

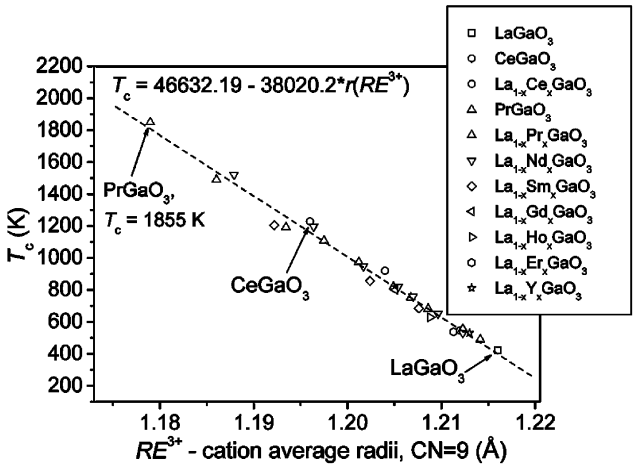


Fig. 10. The temperature dependency of $T_c$ for the *Pbnm* to *R*$\bar{3}$*c* phase transformation in $LaGaO_3$, $CeGaO_3$, $PrGaO_3$, and $La_{1-x}RE_xGaO_3$ solid solutions ($RE$ = Ce, Pr, Nd, Sm, Gd, Ho, Er, Y) versus $RE^{3+}$ cation radius.

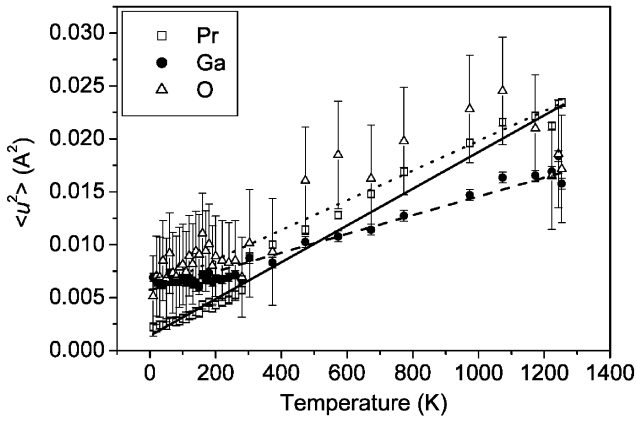


Fig. 11. Temperature evolution of the isotropic displacement parameter of atoms in $PrGaO_3$ structure.

## References

[1] R.L. Sandström, E.A. Giess, W.J. Gallagher, A. Segmüller, E.I. Cooper, M.F. Chisholm, A. Gupta, S. Shinole, R.B. Laibowitz, Appl. Phys. Lett. 53 (1988) 1874.
[2] M. Sasaura, M. Mukaida, S. Miyazawa, Appl. Phys. Lett. 57 (1990) 2728–2729.
[3] S. Miyazawa, M. Sasaura, M. Mukaida, J. Cryst. Growth 128 (1993) 704–708.
[4] H. Dabkowska, A. Dabkowski, J.E. Greedan, J. Cryst. Growth 128 (1993) 699–703.

[5] L. Kebin, Q. Zhenzhong, L. Xijun, Z. Jingsheng, Z. Yuheng, Thin Solid Films 304 (1997) 389–391.
[6] H. Okazaki, A. Arakawa, T. Asahi, O. Oda, K. Aiki, Solid State Electron. 41 (1997) 263–266.
[7] Man Feng, J.B. Goodenough, Eur. J. Solid State Inorg. Chem. 31 (1994) 663–672.
[8] N. Ishihara, H. Matsuda, M. Azmi Bin Bustam, Y. Takita, J. Am. Chem. Soc. 116 (1994) 3801–3803.
[9] N. Ishihara, H. Matsuda, Y. Takita, Solid State Ion. Diffus. React. 86–88 (1996) 197–201.
[10] T. Ishihara, H. Furutani, H. Arikawa, M. Honda, T. Akbay, Y. Takita, J. Electrochem. Soc. 146 (1999) 1643–1649.
[11] W. Marti, P. Fischer, F. Altorfer, H.J. Scheel, M. Tadin, J. Phys.: Condens. Matter 6 (1994) 127–135.
[12] A. Podlesnyak, S. Rosenkranz, F. Fauth, W. Marti, H.J. Sheel, A. Furrer, J. Phys.: Condens. Matter 6 (1994) 4099–4106.
[13] I. Utke, C. Klemenz, H.J. Sheel, P. Nüesch, J. Cryst. Growth 174 (1997) 813–820.
[14] H.M. O'Bryan, P.K. Gallagher, G.W. Berkstresser, C.D. Brandle, J. Mater. Res. 5 (1990) 183–189.
[15] M. Sasaura, S. Miyazawa, J. Cryst. Growth 123 (1992) 126–132.
[16] L. Vasylechko, D. Savytskii, H. Schmidt, U. Bismayer, A. Matkovskii, M. Berkowski, Hasylab Ann. Rep. 1 (2000) 615–616.
[17] L. Vasylechko, Visnyk Lviv Univ. Ser. Khim. 40 (2001) 98–103 (in Ukrainian).
[18] L. Vasylechko, H. Borrmann, M. Berkowski, A. Senyshyn, D. Savytskii, M. Knapp, C. Bähtz, U. Bismayer, A. Matkovskii, Hasylab Ann. Rep. 1 (2002) 433–434.
[19] D. Savytskii, L. Vasylechko, A. Senyshyn, A. Matkovskii, C. Bähtz, M.L. Sanjuan, U. Bismayer, M. Berkowski, Phys. Rev. B 68 (2003) 024101-1–024101-8.
[20] M. Berkowski, J. Fink-Finowicki, P. Byszewski, R. Diduszko, E. Kowalska, R. Aleksijko, W. Piekarczyk, L. Vasylechko, D. Savytskii, L. Perchuć, J. Kapuśniak, J. Cryst. Growth 222 (2001) 194–201.
[21] R.H. Blessing, Acta Crystallogr. A 51 (1995) 33–38.
[22] L.G. Akselrud, P.Yu. Zavalij, Yu. Grin, V.K. Pecharsky, B. Baumgartner, E. Wölfel, Mater. Sci. Forum 133–136 (1993) 335–340.
[23] M. Knapp, V. Joco, C. Bähtz, H.H. Brecht, A. Berghëuser, H. Ehrenberg, H. von Seggern, H. Fuess, Nucl. Instrum. Methods A 521 (2004) 565–570.
[24] C.J. Howard, B.J. Kennedy, J. Phys.: Condens. Matter 11 (1999) 3229–3236.
[25] L. Vasylechko, R. Niewa, W. Schnelle, A. Senyshyn, M. Knapp, Proceedings of the Ninth European Conference on Solid State Chemistry, ECSSC-9. Stuttgart, Germany, September 3–6, 2003, P049.
[26] A. Yoshikawa, A. Saitow, H. Horiuchi, T. Shishido, T. Fukuda, J. Alloys Compd. 266 (1998) 104–110.
[27] T. Hashimoto, N. Tsuzuki, A. Kishi, K. Takagi, K. Tsuda, M. Tanaka, K. Oikawa, T. Kamiyama, K. Yoshida, H. Tagawa, M. Dokija, Solid State Ion. 132 (2000) 183–190.
[28] J.L. Garcia-Munoz, J. Rodriues-Carvajal, P. Lacorre, J.B. Torrance, Phys. Rev. B 46 (8) (1992) 4414–4425.
[29] S. Sasaki, C.T. Prewitt, R.C. Liebermann, Am. Mineral. 68 (1983) 1189–1198.
[30] L. Vasylechko, A. Matkovskii A., D. Savytskii, A. Suchocki, F. Wallrafen, J. Alloys Compd. 292 (1999) 57–65.
[31] M. Berkowski, J. Fink-Finowicki, W. Piekarczyk, L. Perchuc, P. Byszewski, L. Vasylechko, D. Savytskii, K. Mazur, J. Sass, E. Kowalska, J. Kapusniak, J. Cryst. Growth 209 (2000) 75–80.
[32] R. Aleksjko, M. Berkowski, P. Byszewski, B. Dabrowski, R. Diduszko, J. Fink-Finowicki, L. Vasylechko, Cryst. Res. Technol. 36 (2001) 789–800.
[33] L. Vasylechko, R. Niewa, H. Borrmann, M. Knapp, D. Savytskii, A. Matkovskii, U. Bismayer, M. Berkowski, Solid State Ion. 143 (2001) 219–227.
[34] A. Senyshyn, L. Vasylechko, D. Savytskii, C. Bähtz, M. Knapp, U. Bismayer, M. Berkowski, Hasylab Ann. Rep. 1 (2002) 355–356.
[35] R.D. Shannon, Acta Crystallogr. A 32 (1976) 751–767.
[36] B.C. Chakoumakos, Physica B 241–243 (1998) 361–363.